



## Antibacterial effects of iron oxide and silver nanoparticles synthesized by *Bacillus subtilis*: a comparative study

Masoomeh Sasani<sup>a</sup>, Ebrahim Fataei<sup>a,\*</sup>, Reza Safari<sup>a,b</sup>, Fatemeh Nasehi<sup>a</sup>, Marzieh Mosayebi<sup>a</sup>

<sup>a</sup>Department of Environmental Science and Engineering, Ardabil Branch, Islamic Azad University, Ardabil, Iran, Tel. +98 914 354 9400; email: ebfataei@gmail.com (E. Fataei), Tel. +98 911 156 9272; emails: samanehsasani250@yahoo.com (M. Sasani), Tel. +98 914 451 9489; email: fnasehi86@yahoo.com (F. Nasehi), Tel. +98 914 159 3202; email: emailmosayebi@gmail.com (M. Mosayebi)

<sup>b</sup>Caspian Sea Ecology Research Center, Iranian Fisheries Research Institute, Agricultural Research, Education and Extension Organization, Sari, Iran, Tel. +98 911 153 2572; email: safari1351@gmail.com

Received 25 February 2021; Accepted 11 June 2021

### ABSTRACT

The present study aimed to characterize silver and iron oxide nanoparticles (NPs) synthesized by *Bacillus subtilis* for their physicochemical properties and antibacterial activities. The antibacterial properties of NPs were evaluated using agar well diffusion method. In the following, zone of inhibition diameter, minimum inhibitory concentration (MIC), and minimum bactericidal concentration (MBC) were estimated against the standard bacteria of *Staphylococcus aureus* (PTCC 1112), *Bacillus cereus* (PTCC 1015), *Pseudomonas aeruginosa* (PTCC 1074), and *Escherichia coli* (O157:H7). According to the findings, the maximum optical density of Ag NPs and Fe<sub>3</sub>O<sub>4</sub> NPs was read at 435 and 225 nm, respectively, which therefore verified the fabrication of NPs. The shape of Ag NPs was spherical with the size range of 25–45 nm, while the Fe<sub>3</sub>O<sub>4</sub> NPs had cubic and spherical shapes and the size range of 55–80 nm. The results of antimicrobial potentials indicated that the Ag NPs were more active than the Fe<sub>3</sub>O<sub>4</sub> NPs. Also, the biomass synthesis method for both NPs exhibited relatively better physicochemical properties and antimicrobial effects than the supernatant methods. There was a significant difference in antimicrobial effects between selected antibiotics and both synthesized NPs ( $P < 0.05$ ). *S. aureus* and *P. aeruginosa* were the most sensitive and resistant bacteria for both NPs. The MIC values of Ag NPs for *S. aureus* and *P. aeruginosa* were 10 and 40 µg/mL, and the MBC values were 20 and 80 µg/mL, respectively. The obtained properties for the Fe<sub>3</sub>O<sub>4</sub> NPs were weaker than for the Ag NPs, so that the MIC value was 20 µg/mL for *S. aureus* and *B. cereus*, and 40 µg/mL for *E. coli* and *P. aeruginosa*, in addition to, the MBC values were 40 and 80 µg/mL, respectively. Due to the antimicrobial potential of synthesized NPs, they can be used as antimicrobial agents in formulations of various disinfectants and antiseptics, because the used materials possess a very high reactivity due to nanoparticle nature and are able to inhibit unwanted microbial growth during a very short time.

**Keywords:** Silver nanoparticles; Iron oxide nanoparticles; *Bacillus subtilis*; Antibacterial properties; Microbial synthesis

### 1. Introduction

Nanostructures and nanoparticles (NPs) have recently received further attention in various high-tech industries [1], including water and wastewater treatment [2], medicine,

diagnostic techniques [3,4], antimicrobials, pharmaceuticals [5–7] and food industry, owing to their special electrical, optical, magnetic, chemical and mechanical properties [8,9].

Silver (Ag) has been excessively employing in medicine and pharmacy due to its antiseptic and antimicrobial activities. During the production of silver nanoparticles

\* Corresponding author.

(Ag NPs), especially through green synthesis methods, some properties of this metal such as contact surface and dispersion are improved and consequently, the antimicrobial effects of the synthesized fine particles are significantly increased compared to conventional silver [10]. Owing to their small size, the produced NPs easily enter the pathogenic bacteria cells and affect intracellular processes such as the synthesis of DNA, RNA and proteins and thus inhibit microbial growth [11]. In addition to Ag NPs, the fabrication of iron oxide ( $\text{Fe}_3\text{O}_4$ ) NPs is also important due to the changes in its magnetic and electrical properties [12–14].

In recent years, the synthesis of NPs using biological techniques, including fungi, bacteria, and plants have received special attention due to their simplicity, controllability, low-cost, high efficiency, non-toxicity and biocompatibility [14–16]. In this method, when microorganisms are exposed to the metal ion salts, these materials are regenerated through catalytic mechanisms and produced intracellularly or extracellularly [14,17]. The results of antibacterial activities of synthesized NPs have shown a better potential for extracellular NPs to inhibit the growth of pathogenic bacteria compared to intracellular NPs [18]. A study by Hoseynzadeh et al. [19] revealed that *Bacillus cereus* and *Pseudomonas aeruginosa* bacteria isolated from soil had potential to produce Ag NPs with high antimicrobial effects against *S. aureus*, *B. cereus*, *Escherichia coli*, and *Bacillus subtilis* [18,20]. A study by John et al. [21] clearly showed an efficient, rapid synthesis of stable Ag NPs by a new *Pseudomonas* strain with high antimicrobial activity.

The present study was conducted to compare the qualitative properties and antibacterial effects of Ag NPs and  $\text{Fe}_3\text{O}_4$  NPs Produced by *B. subtilis*. By conducting this research and producing eco-friendly metal nanoparticles, novel bio-alternatives can be used to reduce microbial contaminants, especially bacteria. In this way, excessive consumption of chemicals, especially chlorine, which have many environmental consequences, can be avoided. Due to the high reactivity of metal nanoparticles with their very small amounts, the microbial load of indicator bacteria in water can be reduced.

## 2. Materials and methods

### 2.1. Production of nanoparticles

For this study, lyophilized *B. subtilis* was prepared from the microbial collection of Iranian Research Organization for Science and Technology (IROST) and kept in a freezer at  $-18^\circ\text{C}$  for next testing. For bacterial culture, a loop from a pure bacterial colony was transferred to the Luria-Bertani (LB-Merck) broth medium and the sample was completely homogenized using a tube shaker. To enhance the bacterial growth and formation of the growth turbidity, the samples were placed in an incubator at  $30^\circ\text{C}$  for 24 h under aerobic conditions, followed by centrifugation at 5,000 rpm for 20 min. Both supernatant and precipitate containing bacterial biomass were tested for the production of Ag NPs and  $\text{Fe}_3\text{O}_4$  NPs [14]. To produce Ag, and  $\text{Fe}_3\text{O}_4$  NPs using the supernatant, 5 mL of supernatant was mixed with 95 mL of 2 mM silver nitrate solution and placed in a dark place at the room temperature for 48 h (pH = 7). Next, the color change of the solution from yellow to dark brown was the initial

confirmation of Ag NPs, also 2 mM silver nitrate solution without supernatant was considered as a control sample. At the end of the storage period, the color of control sample remained yellow and unchanged. In the next step, to produce the  $\text{Fe}_3\text{O}_4$  NPs, 50 mL of supernatant was added to 50 mL of 2 mM iron oxide ( $\text{Fe}_2\text{O}_3$ ) solution. After adjusting the pH to 8.5, the samples were incubated in the dark at  $35^\circ\text{C}$  and using a shaker at 200 rpm for 5 d. The color change of solution from brick red to black confirmed the initial production of  $\text{Fe}_3\text{O}_4$  NPs; as well as 2 mM iron oxide solution without supernatant was regarded as the control sample [14].

In order to produce Ag NPs and  $\text{Fe}_3\text{O}_4$  NPs using the bacterial biomass, 10 mL of bacterial suspension with an optical density (OD) of 1 at a wavelength of 630 nm was added to 100 mL of 2 mM solutions of silver nitrate and iron oxide, and the same process of nano production method using supernatant was separately repeated for both metals. At this stage, silver nitrate solution and 2 mM iron oxide without bacterial biomass were also used as a control samples [14,22].

After these processes, a 0.22-micron filter paper was applied to separate the Ag NPs and  $\text{Fe}_3\text{O}_4$  NPs produced by both supernatant and biomass methods. Thus, the dark brown supernatants containing Ag NPs and  $\text{Fe}_3\text{O}_4$  NPs were filtered by a Millipore system equipped with a 0.22-micron filter and a vacuum pump and the passed liquid was collected and dried at  $45^\circ\text{C}$ . This process was also run for samples that used biomass to produce NPs, so that after centrifugation at a speed of 6,000 rpm for 6 min (for Ag NPs) and 7,000 rpm for 15 min (for  $\text{Fe}_3\text{O}_4$  NPs), the resulting extracellular NPs in the filtered supernatant were accumulated, filtered and dried similar to the supernatant method [14,22].

A Shimadzu double-beam UV-Vis spectrophotometer (model 1650 PC, Japan) with 1.0 cm quartz cell was used for all spectral measurements. Spectrophotometry method was used to confirm the Ag NPs and  $\text{Fe}_3\text{O}_4$  NPs. Thus, the OD of samples were read in the range of 300–700 nm, and 100–700 nm for Ag NPs and  $\text{Fe}_3\text{O}_4$  NPs, respectively, before drying NPs-containing suspension. To this end, first 200  $\mu\text{L}$  of NPs were added separately to 1,000 mL of distilled water and then their OD values were read at room temperature after preparing the required dilution. Untreated suspensions of silver nitrate and iron oxide in distilled water were also used as the blanks [14,22,23].

Scanning electron microscope (SEM) of the XL Series from Phillips was used to analyze the shape and morphology of produced NPs. First, a certain volume of NPs was centrifuged at 10,000 rpm for 10 min, the supernatant was discarded, the distilled water was poured onto the resulting precipitate and the centrifugation was repeated. This process was performed in triplicate and a certain amount of ethanol 96% was added to the final precipitate and centrifugation was repeated similar to the previous steps. After discarding the supernatant, the resulting precipitate was dried at  $40^\circ\text{C}$  for 48 h and prepared for SEM imaging, followed by measuring the size of NPs to calculate the mean size and recording their morphology [14,23].

### 2.2. Evaluation of antibacterial effects

The antibacterial properties of produced Ag NPs and  $\text{Fe}_3\text{O}_4$  NPs were examined on the standard bacteria of

*S. aureus* (PTCC 1112), *B. cereus* (PTCC 1015), *P. aeruginosa* (PTCC 1074) and *E. coli* (O157H7) prepared from the microbial collection of IROST.

The antibacterial activities were measured by agar well diffusion method. For this purpose, 20  $\mu\text{L}$  of studied bacterial suspension (containing  $1.5 \times 10^8$  CFU/ml equivalent to 0.5 McFarland standard turbidity) was cultured onto Mueller Hinton agar medium. The concentrations to measure the zone of inhibition (ZOI) diameter were 50 and 100  $\mu\text{g}/\text{mL}$  of Ag NPs and  $\text{Fe}_3\text{O}_4$  NPs, which were poured into 7 mm wells created on the medium after the sonication at a frequency of 40 kHz for 30 min. The purpose of sonication of NPs solutions was to diffuse them evenly and preparation of a homogeneous suspensions. The tests were separately performed for Ag NPs and  $\text{Fe}_3\text{O}_4$  NPs synthesized from the supernatant and bacterial biomass. The ampicillin (for gram-positive bacteria) and gentamicin (for gram-negative bacteria) antibiotics were utilized as the positive control and 4% dimethyl sulfoxide (DMSO) as the negative control. After incubating the samples at 35°C for 24 h, the ZOI diameter was measured in millimeters [22,24].

The microdilution method was performed to determine the minimum inhibitory concentration (MIC) and minimum bactericidal concentration (MBC). First, the initial stocks of Ag NPs and  $\text{Fe}_3\text{O}_4$  NPs were prepared; 1 mg of NPs was added to 10 mL of normal saline and sonicated at 40 kHz for 30 min (equivalent to 100  $\mu\text{g}/\text{mL}$ ). Then, the serial dilutions were prepared in different tubes as 2.5, 5, 10, 20, 40, and 80  $\mu\text{g}/\text{mL}$ , respectively. After adding 20  $\mu\text{L}$  of pre-prepared bacterial suspension and 1 mL of Tryptic Soy Broth (TSB) medium to each tube, the samples were incubated at 35°C for 24 h. The control groups in this experiment included the positive control (medium without Ag NPs or  $\text{Fe}_3\text{O}_4$  NPs and only with bacteria) and the negative control (medium with Ag NPs or  $\text{Fe}_3\text{O}_4$  NPs and without bacteria). The lowest concentration of nanoparticle suspension, in which no turbidity was observed, was considered as MIC value. MIC dilutions of 10  $\mu\text{L}$  or more were cultured onto TSB medium and, after incubation at 35°C for 24 h, the lowest concentration that could reduce the bacterial growth by 99.99% was considered as MBC value [24–26].

Attained data were analyzed by SPSS Version 20 software. One-way analysis of variance (ANOVA) test was applied to evaluate the production of Ag NPs and  $\text{Fe}_3\text{O}_4$  NPs and their antimicrobial effects. The mean comparison was performed by Duncan's test at a significance level of 5%. All data were reported as mean  $\pm$  standard deviation (SD) and analyses were conducted in triplicate.

### 3. Results and discussion

Techniques of UV-vis spectrophotometry, SEM, X-ray diffraction (XRD), and Fourier-transform infrared spectroscopy (FTIR) were employed to verify the produced NPs. The maximum OD value for Ag NPs and  $\text{Fe}_3\text{O}_4$  NPs was observed at 435 and 225 nm, respectively, thereby confirming the synthesized NPs. In a study by Maghsoudy et al. [23] on the production of Ag NPs and  $\text{Fe}_3\text{O}_4$  NPs using the *Erodium cicutarium* plant extract, the highest read wavelengths were 420 and 230 nm, respectively, which is consistent with our findings.

In a study by Sundaram et al. [14] on the production of  $\text{Fe}_3\text{O}_4$  NPs using *B. subtilis*, the maximum OD value was achieved at 250–350 nm, indicating the production of  $\text{Fe}_3\text{O}_4$  NPs and its uniform dispersion. Mahmoud et al. [24] reported that the maximum wavelength for Ag NPs was 430 nm, consistent with the present study. Also, Begam [27] recorded a wavelength of 420 nm for Ag NPs synthesized by marine bacteria. The maximum OD value read for  $\text{Fe}_3\text{O}_4$  NPs was 220 nm in a study of Ghani et al. [28], which is in accordance with the present study.

The SEM images showed that the produced Ag NPs had a regular spherical shape; however, other shapes were also observed sporadically. The mean size of Ag NPs was 25–45 nm and 80% of which were in this range (Fig. 1a). The produced  $\text{Fe}_3\text{O}_4$  NPs were in spherical and cubic shapes as well as other irregular shapes sporadically. Some agglomerated particle was observed in the microscopic imaging of nanoparticles produced; however, there was no direct contact between the particles due to their relative stability [29,30]. The stability of the produced nanoparticles can be attributed to the synthesis of secondary metabolites with the nature of the bacterial protein that coated the nanoparticles, thus resulting in stability. The mean size of  $\text{Fe}_3\text{O}_4$  NPs was 55–80 nm and most of them were in this range (Fig. 1b). Sundaram et al. [14], Begam [27] and Ghani et al. [28] reported similar results; the particle size was measured to be < 100 nm and that the produced NPs had different ranges depending on the used microbial strains. The particle shapes in these studies were mostly spherical to cubic forms.

The XRD pattern of the synthesized NPs are shown in Fig. 2. Analysis of XRD results of Ag NPs synthesized by *B. subtilis* confirmed crystalline nature of Ag NPs and demonstrated some characteristic peaks at 28.53°, 32.03°, 40.83°, and 45.58° two theta ( $2\theta$ ) values that corresponds to (210), (113), (141), and (124) facets of silver NPs, respectively. Also, for iron oxide NPs according to Fig. 2b, the main characteristic peaks appear at 31.78°, 38.33°, 45.63°, and 56.63°  $2\theta$  values that corresponds to (220), (311), (400), and (511) facets of  $\text{Fe}_3\text{O}_4$  NPs, respectively [18,20].

FTIR spectra of synthesized silver NPs is shown in Fig. 3a. FTIR analysis confirmed the existence of bacterium metabolites, which are responsible for the reduction of Ag(I) ions into Ag(0) NPs. It was used to identify the characteristic functional groups involved in the formation of Ag NPs. The FTIR spectral peaks appeared at 3,424.33  $\text{cm}^{-1}$  assigned to the hydroxyl (–O–H) and amine (–N–H) stretching due to the presence of amines and water. Peaks at 2,962.70 and 1,647.24  $\text{cm}^{-1}$  are due to vibrations of C–H and (NH) C=O stretching of alkanes and (amine) amide bonds associated with the protein molecules, respectively. A peak at 1,111.22  $\text{cm}^{-1}$  is due to vibrations of C–O stretching of alcoholic groups. The peak near 995  $\text{cm}^{-1}$  assigned to C=CH<sub>2</sub> and the peaks at 621.39 and 540.02  $\text{cm}^{-1}$  were attributed to CH out of plane bending vibrations which are substituted ethylene systems –CH=CH (cis) [18]. Therefore, the bioreduction of silver (I) into Ag NPs may be attributed to the presence of phenols, proteins, amino groups, alkanes, and alkenes present in the *B. subtilis*.

FTIR spectra of synthesized iron oxide NPs using *B. subtilis* is presented in Fig. 3b. Peaks at 3,399.76  $\text{cm}^{-1}$  is

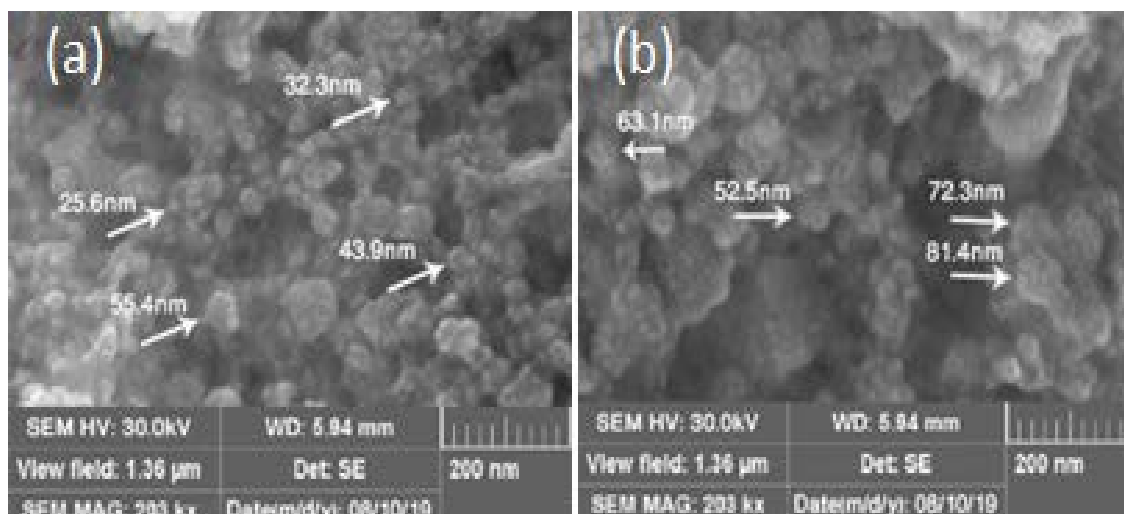


Fig. 1. SEM images of (a) silver NPs and (b) iron oxide NPs synthesized by *Bacillus subtilis*.

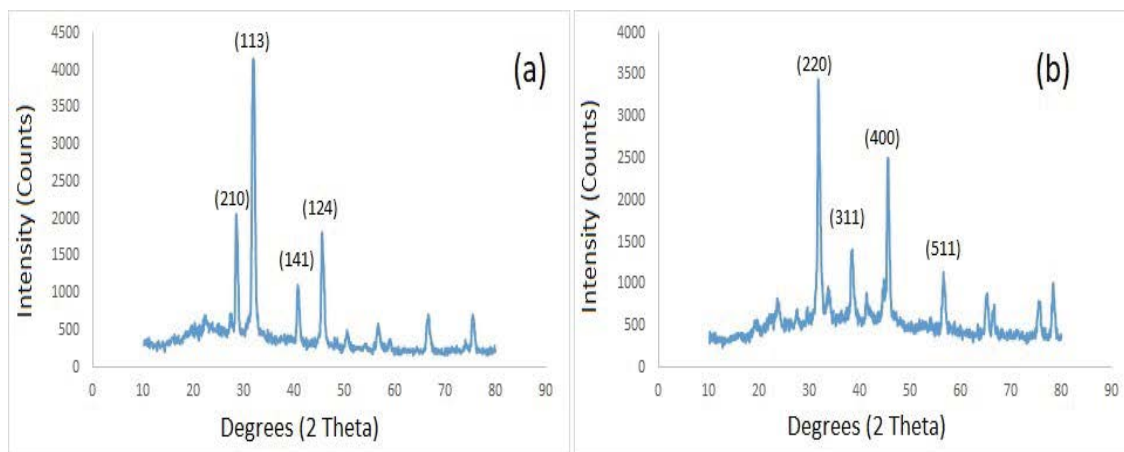


Fig. 2. XRD pattern of (a) silver NPs and (b) iron oxide NPs synthesized by *Bacillus subtilis*.

assigned to the OH stretching of alcohols and phenols [12]. A peak at  $2,963.83\text{ cm}^{-1}$  indicate the presence of CH stretching groups. The absorption peak at  $1,674.79\text{ cm}^{-1}$  can be assigned to the amide band of proteins arising from carbonyl stretching in proteins. The peak at  $1,387.26\text{ cm}^{-1}$  may be assigned to the presence of carboxylate ions ( $\text{COO}^-$ ), which is responsible for the formation of iron oxide NPs. The formation of  $\text{Fe}_3\text{O}_4$  NPs is characterized by the absorption band at  $536.50\text{ cm}^{-1}$  which is correspond to the Fe–O bond [12,13].

### 3.1. Evaluation of antibacterial effects

#### 3.1.1. Measurement of ZOI diameter

The results of assessing antimicrobial effects of Ag NPs using agar well diffusion method fabricated from *B. subtilis* by the two approaches are shown in Table 1. Recently, agar well diffusion method is widely used to evaluate the antimicrobial activity of plants or microbial extracts. As can be seen, the biomass method was relatively more effective than the supernatant method, exhibiting better

antibacterial activities on the study bacteria; however, in most cases, there was no significant difference between the data. The difference in the antimicrobial effects between selected antibiotics and Ag NPs was significant ( $P < 0.05$ ). Among these, *S. aureus* was the most sensitive and *P. aeruginosa* was the most resistant bacteria. In general, gram-positive bacteria were more sensitive to antimicrobials than gram-negative ones, probably due to the presence of lipopolysaccharide and lipid layers in the wall structure of gram-negative bacteria; this is not always true and gram-positive bacteria can also be more resistant in some cases.

In the same way, evaluation results of antimicrobial effects of  $\text{Fe}_3\text{O}_4$  NPs using agar well diffusion method fabricated from *B. subtilis* by the two approaches are summarized in Table 2. Similarly, obtained results showed that the biomass method was relatively more effective than the supernatant method, exhibiting better antibacterial activities on the study bacteria, like the findings of Ag NPs, and in most cases, no significant difference was observed between the data. The difference in the antimicrobial effects between the selected antibiotics and  $\text{Fe}_3\text{O}_4$  NPs was significant ( $P < 0.05$ ).

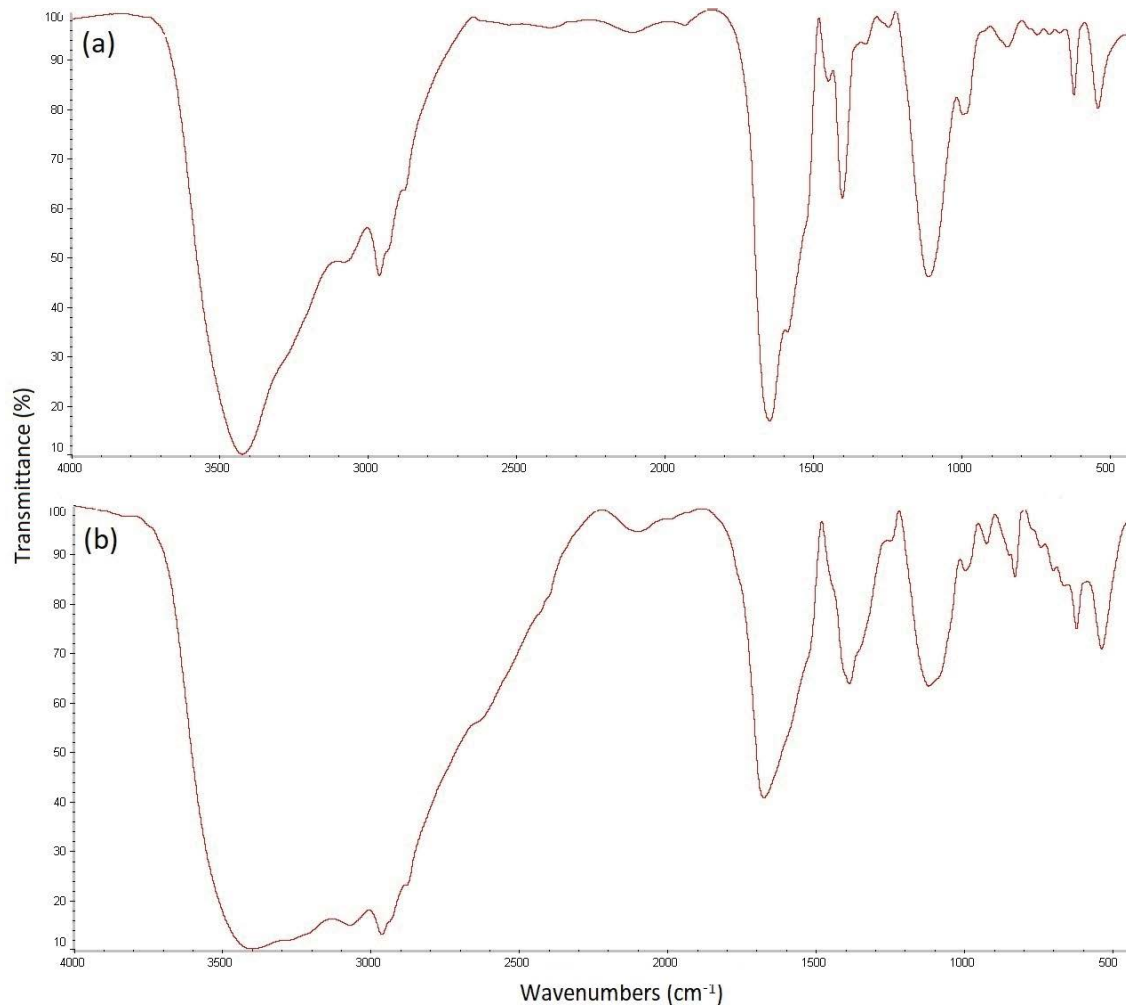


Fig. 3. FTIR spectra of (a) silver NPs and (b) iron oxide NPs synthesized by *Bacillus subtilis*.

Table 1

Zone of inhibition diameter (mm) for two concentrations of silver nanoparticles extracted from supernatant content and biomass of *Bacillus subtilis* against indicator bacteria using agar well diffusion method

Bacteria	Synthesis method	50 µg/mL	100 µg/mL	Ampicillin	Gentamicin	Silver nitrate
<i>Staphylococcus aureus</i>	S	18 ± 0.5cA	25 ± 0.5bA	30 ± 0.5a	–	10 ± 0.2dA
	B	19 ± 0.2cA	25 ± 0.3bA	30 ± 0.5a	–	10 ± 0.2dA
<i>Bacillus cereus</i>	S	11 ± 0.1cBC	14 ± 0.5bBC	26 ± 0.2a	–	10 ± 0.1cA
	B	13 ± 0.3cB	15 ± 0.2bB	26 ± 0.2a	–	10 ± 0.1dA
<i>Pseudomonas aeruginosa</i>	S	9 ± 0.1cD	13 ± 0.1bCD	–	18.5 ± 0.3a	7 ± 0.2cAB
	B	9 ± 0.2cD	14 ± 0.3bBC	–	18.5 ± 0.3a	7 ± 0.2cAB
<i>Escherichia coli</i>	S	12 ± 0.3cB	15 ± 0.2bB	–	24 ± 0.2a	9 ± 0.1dA
	B	14 ± 0.1cB	17 ± 0.4bB	–	24 ± 0.2a	9 ± 0.1dA

S = synthesis by supernatant; B = synthesis by biomass; also, different capital and lowercase letters in each row and column show the significant difference between the data ( $P < 0.05$ ).

Among the study bacteria, *S. aureus* and *P. aeruginosa* were the most sensitive and the most resistant bacteria, respectively. According to the results, the antimicrobial effects of Ag NPs were stronger than  $\text{Fe}_3\text{O}_4$  NPs.

Today, silver nitrate is used as a common antimicrobial agent because it has bacteriostatic and bactericidal effects

on most pathogenic and indicator bacteria. When Ag NPs are produced from silver salts, their antimicrobial effects are greatly increasing due to their very high reactivity and higher contact surface. Ordinary iron oxide has no antimicrobial effect, but its nanoparticle shape has antimicrobial properties and inhibits further growth of indicator

bacteria. Thus, the greater activity in inhibiting of bacterial growth by Ag NPs is due to the inherent antimicrobial potential of silver metal, which increases after conversion to NPs [31–33].

### 3.1.2. Determination of MIC and MBC values

The MIC and MBC calculated values of Ag NPs and Fe<sub>3</sub>O<sub>4</sub> NPs against indicator bacteria are shown in Tables 3 and 4. The outcomes of microdilution tests of the synthesized particles with both supernatant and biomass were the same. The results showed that the MIC values of silver NPs for *S. aureus* and *P. aeruginosa* were 10 and 40 µg/mL, respectively and the MBC values of Ag NPs for these two bacteria were 20 and 80 µg/mL, respectively; which, like the results of agar well diffusion method, indicated the high resistance of *P. aeruginosa* and sensitivity of *S. aureus* to the concentrations of Ag NPs used. Results showed that the bacteriostatic and bactericidal effects of Fe<sub>3</sub>O<sub>4</sub> NPs on indicator bacteria were weaker than Ag NPs; so that the MIC value was 20 µg/mL for *S. aureus* and *B. cereus*, and 40 µg/mL for *E. coli* and *P. aeruginosa*; as well as the MBC values were 40 and 80 µg/mL, respectively.

In a study by Maghsoudy et al. [23] the MIC values of Fe<sub>3</sub>O<sub>4</sub> NPs and Ag NPs prepared from *Cicutarium erodium* plant extract were 397.38 and 399.53 µg/mL against *E. coli* and *S. aureus*, respectively. In latter study, the antimicrobial effect of Fe<sub>3</sub>O<sub>4</sub> NPs was reported to be slightly higher than that of Ag NPs. Comparing the above results with the present study, it was found that the MIC value of NPs synthesized by the plant is probably much higher than the bacterium due to the nature of the production of NPs, and is fulfilled by different mechanisms. In a study by Garmasheva et al. [22] Ag NPs produced by *Lactobacillus plantarum* at a concentration of 50 g/L had a suitable effect on most of the studied bacteria. In their report, ZOI diameter of *S. aureus* was larger than the other bacteria and that *Salmonella enteritidis* was more resistant than the others. The results of ZOI diameter for indicator bacteria were similar to the present study.

In a study on the effects of Ag NPs on some pathogenic bacteria, Begam [27] showed that a concentration of 30 mg/µL has more antimicrobial effects than a concentration of

15 mg/µL. Among the study bacteria, *Salmonella typhimurium* was the most sensitive (with a ZOI diameter of 15 mm), and *Klebsiella pneumoniae* was the most resistant bacterium.

In a study by Ghani et al. [28] the results of inhibitory effect revealed that the iron nitrate NPs have higher antimicrobial effects, while the normal form of iron (iron nitrate) showed no antimicrobial effects. Among the study bacteria, *E. coli* and *P. aeruginosa* were more sensitive than the others, which is inconsistent with the present study. The results of MIC and MBC tests were similar to those from the ZOI test, and concentrations of 0.015 and 0.0078 mg/L inhibited the growth of *P. aeruginosa* and *E. coli*, respectively. However, a concentration of 0.031 mg/mL inhibited the growth of *B. cereus* and *S. aureus*, which contradicts the present study.

Table 3  
Results of minimum inhibitory concentration (MIC) and minimum bactericidal concentration (MBC) of silver nanoparticles extracted from supernatant content and biomass of *Bacillus subtilis* against indicator bacteria using microdilution method

Bacteria	MIC (µg/mL)	MBC (µg/mL)
<i>Staphylococcus aureus</i>	10	20
<i>Bacillus cereus</i>	20	40
<i>Pseudomonas aeruginosa</i>	40	80
<i>Escherichia coli</i>	20	40

Table 4  
Results of minimum inhibitory concentration (MIC) and minimum bactericidal concentration (MBC) of iron oxide nanoparticles extracted from supernatant content and biomass of *Bacillus subtilis* against indicator bacteria using microdilution method

Bacteria	MIC (µg/mL)	MBC (µg/mL)
<i>Staphylococcus aureus</i>	20	40
<i>Bacillus cereus</i>	20	40
<i>Pseudomonas aeruginosa</i>	40	80
<i>Escherichia coli</i>	40	80

Table 2  
Zone of inhibition diameter (mm) for two concentrations of iron oxide nanoparticles extracted from supernatant content and biomass of *Bacillus subtilis* against indicator bacteria using agar well diffusion method

Bacteria	Synthesis method	50 µg/mL	100 µg/mL	Ampicillin	Gentamicin	Iron oxide
<i>Staphylococcus aureus</i>	S	13.5 ± 0.3cA	17 ± 0.1bB	30 ± 0.5a	–	0
	B	14.2 ± 0.4cA	19.5 ± 0.6bA	30 ± 0.5a	–	0
<i>Bacillus cereus</i>	S	10.5 ± 0.3cB	12.6 ± 0.4bCD	26 ± 0.2a	–	0
	B	11 ± 0.4cB	13.2 ± 0.3bC	26 ± 0.2a	–	0
<i>Pseudomonas aeruginosa</i>	S	7.5 ± 0.2cC	10 ± 0.1bE	–	18.5 ± 0.3a	0
	B	8.2 ± 0.4cC	11.3 ± 0.1bDE	–	18.5 ± 0.3a	0
<i>Escherichia coli</i>	S	10 ± 0.4cB	13.5 ± 0.5bC	–	24 ± 0.2a	0
	B	10.2 ± 0.3cB	14.3 ± 0.4bC	–	24 ± 0.2a	0

S = synthesis by supernatant; B = synthesis by biomass; also, different capital and lowercase letters in each row and column show the significant difference between the data ( $P < 0.05$ ).

The results of a study by Mahmoud et al. [24] on the effect of Ag NPs produced by *Bacillus pumilus* on some opportunistic pathogenic bacteria using the determination of ZOI diameter, MBC, and MIC values showed that *S. aureus* and *Shigella* were more sensitive than other species and the ZOI diameter was between 25 and 30 mm. The results of ZOI diameter measurement in *S. aureus* were consistent with the present study, however, *P. aeruginosa* with a ZOI diameter of 23 mm was reported to be a relatively sensitive bacterium that contradicted the present study. The MIC and MBC results for most bacteria, except for *E. coli*, were between 5 and 15  $\mu\text{g}/\text{mL}$ , which were slightly lower than in the present study, probably due to the nature of the nano-production and the nanoparticle size. In the study of Mahmoud et al. [24] on the synthesis of iron NPs using *Alternaria* fungi, it was found that the results of measuring ZOI diameter for the selected bacteria are similar to our study, so that *P. aeruginosa* and *B. cereus* are more resistant and sensitive than the others, respectively.

#### 4. Conclusions

The results of the present study indicated that *B. subtilis* is able to produce nanoparticles from two metal solutions of silver and iron, so that the synthesized nanoparticles showed the highest wavelengths in the range of 435 and 225 nm, respectively. The scanning electron microscopy images exhibited that the silver nanoparticles have smaller size and spherical shape, however iron oxide nanoparticles have larger size and spherical to cubic shapes. The XRD pattern of NPs synthesized by *B. subtilis* well confirmed the crystalline nature of Ag NPs and iron oxide NPs. The FTIR analysis indicated that bioreduction of silver (I) into Ag NPs may be attributed to the presence of phenols, proteins, amino groups, alkanes, and alkenes present in the *B. subtilis*. Also, the formation of  $\text{Fe}_3\text{O}_4$  NPs is characterized by the absorption band at  $536.50\text{ cm}^{-1}$  which is correspond to the Fe–O bond. The analysis of antimicrobial effects revealed that there is no significant difference in the antimicrobial activities between nanoparticles synthesized from supernatant content and biomass. In general, silver nanoparticles have better antimicrobial potential than iron oxide nanoparticles, and *S. aureus* and *P. aeruginosa* are the most sensitive and resistant bacteria, respectively. Due to the antimicrobial effects of these nanoparticles, they can be used as bio-alternatives and eco-friendly nanomaterials to reduce microbial contaminants, especially indicator bacteria in water, and contribute to the health and food safety of society.

#### Acknowledgement

This article was extracted from a Ph.D. Degree Thesis. The authors of this paper are sincerely grateful to the Islamic Azad University of Ardabil, Iran for providing the financial and academic support to the project.

#### References

- [1] R. Razavi, S.M. Abrishamifar, G.E. Rajaei, M.R.R. Kahkha, M. Najafi, Theoretical investigation of the use of nanocages with an adsorbed halogen atom as anode materials in metal-ion batteries, *J. Mol. Model.*, 24 (2018) 1–9, doi: 10.1007/s00894-018-3604-0.
- [2] S. Khalili Arjaghi, G. Ebrahimzadeh Rajaei, N. Sajjadi, M. Kashefi Alasl, E. Fataei, Removal of mercury and arsenic metal pollutants from water using iron oxide nanoparticles synthesized from Lichen *Sinensis Ramalina* Extract, *J. Health*, 11 (2020) 397–408.
- [3] W. Gao, S. Milad Abrishamifar, G. Ebrahimzadeh Rajaei, R. Razavi, M. Najafi, DFT study of cyanide oxidation on surface of Ge-embedded carbon nanotube, *Chem. Phys. Lett.*, 695 (2018) 44–50.
- [4] K.D. Karjabad, S. Mohajeri, A. Shamel, M. Khodadadi-Moghaddam, G.E. Rajaei, Boron nitride nanoclusters as a sensor for Cyclosarin nerve agent: DFT and thermodynamics studies, *SN Appl. Sci.*, 2 (2020) 1–8.
- [5] A. Behmanesh, F. Salimi, G.E. Rajaei, Adsorption behavior of letrozole on pure, Ge- and Si-doped  $\text{C}_{60}$  fullerenes: a comparative DFT study, *Monatsh. Chem.*, 151 (2020) 25–32.
- [6] E. Golipour-Chobar, F. Salimi, G.E. Rajaei, Boron nitride nanocluster as a carrier for lomustine anticancer drug delivery: DFT and thermodynamics studies, *Monatsh. Chem.*, 151 (2020) 309–318.
- [7] F. Kamali, G. Ebrahimzadeh Rajaei, S. Mohajeri, A. Shamel, M. Khodadadi-Moghaddam, Adsorption behavior of metformin drug on the  $\text{C}_{60}$  and  $\text{C}_{48}$  nanoclusters: a comparative DFT study, *Monatsh. Chem.*, 151 (2020) 711–720.
- [8] E. Rezaei-Aghdam, A. Shamel, M. Khodadadi-Moghaddam, G.E. Rajaei, S. Mohajeri, Synthesis of  $\text{TiO}_2$  and ZnO Nanoparticles and CTAB-Stabilized  $\text{Fe}_3\text{O}_4$  nanocomposite: kinetics and thermodynamics of adsorption, *Res. Chem. Intermed.*, 47 (2021) 1759–1774.
- [9] P. Singh, H. Singh, Y.J. Kim, R. Mathiyalagan, C. Wang, D.C. Yang, Extracellular synthesis of silver and gold nanoparticles by *Sporosarcina koreensis* DC4 and their biological applications, *Enzyme Microb. Technol.*, 86 (2016) 75–83.
- [10] S. Kaviya, J. Santhanalakshmi, B. Viswanathan, J. Muthumary, K. Srinivasan, Biosynthesis of silver nanoparticles using Citrus sinensis peel extract and its antibacterial activity, *Spectrochim. Acta, Part A*, 79 (2011) 594–598.
- [11] S.-H. Kim, H.-S. Lee, D.-S. Ryu, S.-J. Choi, D.-S. Lee, Antibacterial activity of silver-nanoparticles against *Staphylococcus aureus* and *Escherichia coli*, *Korean J. Microb. Biotechnol.*, 39 (2011) 77–85.
- [12] S.K. Arjaghi, M.K. Alasl, N. Sajjadi, E. Fataei, G.E. Rajaei, Green synthesis of iron oxide nanoparticles by R5 lichen extract and its application in removing heavy metals of lead and cadmium, *Biol. Trace Elem. Res.*, 199 (2021) 763–768.
- [13] G.E. Rajaei, S. Khalili-Arjaghi, E. Fataei, N. Sajjadi, M. Kashefi-Alasl, Fabrication and characterization of polymer-based nanocomposite membrane modified by magnetite nanoparticles for  $\text{Cd}^{2+}$  and  $\text{Pb}^{2+}$  removal from aqueous solutions, *C.R. Chim.*, 23 (2020) 563–574.
- [14] P.A. Sundaram, R. Augustine, M. Kannan, Extracellular biosynthesis of iron oxide nanoparticles by *Bacillus subtilis* strains isolated from rhizosphere soil, *Biotechnol. Bioprocess Eng.*, 17 (2012) 835–840.
- [15] J.R. Chen, Y.Q. Miao, N.Y. He, X.H. Wu, S.J. Li, Nanotechnology and biosensors, *Biotechnol. Adv.*, 22 (2004) 505–518.
- [16] A. Nanda, M. Saravanan, Biosynthesis of silver nanoparticles from *Staphylococcus aureus* and its antimicrobial activity against MRSA and MRSE, *Nanomed. Nanotechnol. Biol. Med.*, 5 (2009) 452–456.
- [17] A. Ahmad, P. Mukherjee, S. Senapati, D. Mandal, M.I. Khan, R. Kumar, M. Sastry, Extracellular biosynthesis of silver nanoparticles using the fungus *Fusarium oxysporum*, *Colloids Surf., B*, 28 (2003) 313–318.
- [18] E. Keikha, A. Emamjomeh, B. Fakheri, Biosynthesis of silver nanoparticles using aqueous extract of *Withania somnifera*, *Modares J. Biotechnol.*, 11 (2020) 225–232.
- [19] A. Hoseynzadeh, M. Khaleghi, H. Sasan, Investigating the antimicrobial effects of silver nanoparticles synthesized by bacteria isolated from agricultural soils of Kerman, Iran, *J. Med. Microbiol.*, 11 (2017) 136–148.
- [20] R. Safarkar, G. Ebrahimzadeh Rajaei, S. Khalili-Arjaghi, The study of antibacterial properties of iron oxide nanoparticles

- synthesized using the extract of lichen *Ramalina sinensis*, Asian J. Nanosci. Mater., 3 (2020) 157–166.
- [21] M.S. John, J.A. Nagoth, K.P. Ramasamy, A. Mancini, G. Giuli, A. Natalello, P. Ballarini, C. Miceli, S. Pucciarelli, Synthesis of bioactive silver nanoparticles by a *Pseudomonas* strain associated with the antarctic psychrophilic protozoon *Euplotes focardii*, Mar. Drugs, 18 (2020) 38, doi: 10.3390/md18010038.
- [22] I. Garmasheva, N. Kovalenko, S. Voychuk, A. Ostapchuk, O. Livins'ka, L. Oleschenko, *Lactobacillus* species mediated synthesis of silver nanoparticles and their antibacterial activity against opportunistic pathogens *in vitro*, BioImpacts: BI, 6 (2016) 219–223.
- [23] N. Maghsoudy, P.A. Azar, M.S. Tehrani, S.W. Husain, K. Larijani, Biosynthesis of Ag and Fe nanoparticles using *Erodium cicutarium*; study, optimization, and modeling of the antibacterial properties using response surface methodology, J. Nanostruct. Chem., 9 (2019) 203–216.
- [24] W.M. Mahmoud, T.S. Abdelmoneim, A.M. Elazzazy, The impact of silver nanoparticles produced by *Bacillus pumilus* as antimicrobial and nematicide, Front. Microbiol., 7 (2016) 1746, doi: 10.3389/fmicb.2016.01746.
- [25] K. Gudikandula, S. Charya Maringanti, Synthesis of silver nanoparticles by chemical and biological methods and their antimicrobial properties, J. Exp. Nanosci., 11 (2016) 714–721.
- [26] M. Omrani, E. Fataei, Synthesizing colloidal zinc oxide nanoparticles for effective disinfection; impact on the inhibitory growth of *Pseudomonas aeruginosa* on the surface of an infectious unit, Pol. J. Environ. Stud., 27 (2018) 1639–1645.
- [27] J. Begam, Biosynthesis and characterization of silver nanoparticles (AgNPs) using marine bacteria against certain human pathogens, Int. J. Adv. Sci. Res., 2 (2016) 152–156.
- [28] S. Ghani, B. Rafiee, D. Sadeghi, M. Ahsani, Biosynthesis of iron nano-particles by *Bacillus Megaterium* and its anti-bacterial properties, J. Babol Univ. Med. Sci., 19 (2017) 13–19.
- [29] G. Ebrahimzadeh Rajaei, H. Aghaie, K. Zare, M. Aghaie, Adsorption of Ni(II) and Cd(II) ions from aqueous solutions by modified surface of *Typha latifolia* L. root, as an economical adsorbent, J. Phys. Theor. Chem., 9 (2012) 137–147.
- [30] G.E. Rajaei, H. Aghaie, K. Zare, M. Aghaie, Adsorption of Cu(II) and Zn(II) ions from aqueous solutions onto fine powder of *Typha latifolia* L. root: kinetics and isotherm studies, Res. Chem. Intermed., 39 (2013) 3579–3594.
- [31] F.R. Abdul, H.T. Subhi, N.A. Taher, I.A. Raheem, Activity of iron oxide nanoparticles on bacterial biofilm formation, Int. J. Pharm. Sci. Res., 11 (2019) 1126–1130.
- [32] A. Matei, S. Matei, G.-M. Matei, G. Cogălniceanu, C.P. Cornea, Biosynthesis of silver nanoparticles mediated by culture filtrate of lactic acid bacteria, characterization and antifungal activity, The EuroBiotech J., 4 (2020) 97–103.
- [33] R. Mohammadi Aloucheh, O. Baris, A. Asadi, S. Gholam Zadeh, M. Kharat Sadeghi, Characterization of Aquatic Beetles Shells (Hydraenidae family) derived chitosan and its application in order to eliminate the environmental pollutant bacterial, Anthropogenic Pollut. J., 3 (2019) 43–48.